RESPONSE OF BRIDGES TO STEADY AND RANDOM WIND LOAD
Wind analysis of the Hardanger Supsension Bridge

Andreas Domaingo [a], Johann Stampler [a], Dorian Janjic [a]

[a] TDV Technische Datenverarbeitung/Bentley Systems, Graz, Austria

INTRODUCTION

With more and more increasing span lengths of bridges due to better material quality and improved construction techniques new effects must be included in the design process. A major issue is the increased susceptibility of such structures to wind induced vibrations. Especially steel bridges – and consequently a majority of suspension and cable stayed bridges – allow for extraordinary slender main girder cross section. The price to pay for these material savings and architectural highlights is a balancing act concerning the wind design, because one can no longer state a priori that the final construction will withstand the acting wind forces. Instead, sophisticated analysis methods must be applied to determine critical wind velocities for all types of known wind effects.
By considering the typical cross section of modern long-span bridges a close resemblance to aircraft wings is obvious. Therefore, many analysis techniques originally applied in aeronautics have crossed over to bridge engineering. Although many problems can be reduced to simplified models there are some aspects which can only be treated numerically by referring to sophisticated computer models – a field of activity which is nowadays often called Computational Wind Engineering (CWE) [1]. This term comprises the characterization of interaction of wind and cross-section by numerical Computational Fluid Dynamics (CFD) methods on the one hand, and structural analysis based on the resulting aerodynamic coefficients on the other. This so-called wind buffeting analysis must take into account the random properties of wind events, which are described by wind power spectrum and coherence. On the other hand, detailed information of the considered structure must be provided, which is done in the form of eigenmodes and –frequencies. This information is combined in a statistical analysis method to provide information about the structure peak response due to a given wind profile.
In this paper the application of CWE methods is presented for the investigation of the Hardanger bridge, a suspension bridge planned in Norway. First, detailed CFD calculations are performed to obtain an aerodynamic characterization of the used cross sections for main deck and pylons. The obtained information is used in the following to perform wind buffeting calculations for the prediction of response to fluctuating wind. All calculations were performed with a commercial software package which is capable of CFD calculations [2, 3] as well as wind buffeting analysis [4].

1 HARDANGER BRIDGE

The planned Hardanger bridge will be a suspension bridge with a main span of 1310 m and a total length of 1380 m which crosses the Hardanger fjord in Norway. It will be number one in Norway and seven world wide. The opening is planned for 2011. The main deck will be 18.3 m wide, including two driving lanes and a separated cyclist and pedestrian path. The Pylons will be more than 180 m high and the maximum clearance for ship vessels will be around 50 m.
The very large ratio of main span to side spans is due to the fact that the shore of the fjord drops very deeply, so that the pylons must be placed close to the water side. The construction will be done by lifting the individual girder segments and temporary connection to each other with hinges. Once all elements are lifted the final welding will be performed. During this time, the main girder will be even more susceptible to wind induced vibrations.
The cable lengths for main cable and hangers were calculated by software by applying a set of constraints for sag and cable forces [5] for the bridge in service state. The final geometry of the main girder will not be straight but with a constant radius in elevation. This vertical radius is

achieved by a constant bending moment induced between the pylons and the hangers closest to the pylons.

2 AERODYNAMIC CHARACTERIZATION

Numerical investigations of the main girder and pylons were performed with a CFD module [2] which applies the vortex particle method to describe the air flow around the cross-section. Large scale wind tunnel measurements were carried out in Denmark. Additionally, small scale wind tunnel measurements were done in collaboration with The Virtual Vehicle Competence Center (vif) in Graz to calibrate the developed CFD module [6].

First, the steady state coefficients of the main deck were investigated for a plain deck configuration as indicated in *Fig. 1*. For comparison, wind tunnel measurements with a 1:100 model of the deck are also given. Within the wind tunnel, wind velocities up to 7 m/s were admissible, which corresponds to Reynolds number of about 10^5. The CFD calculations were performed for the same Reynolds number, compared to > 10^7 for the full scale situation. Further investigations showed that the results show almost no dependency on the Reynolds number. The coefficients for drag (*D*), lift (*L*) and moment (*M*) were normalized according to

$$C_D = \frac{D}{\frac{1}{2}\rho U_\infty^2 H} \qquad C_L = \frac{L}{\frac{1}{2}\rho U_\infty^2 B} \qquad C_M = \frac{M}{\frac{1}{2}\rho U_\infty^2 B^2} \tag{1}$$

where *B* and *H* are width and height of the cross section respectively, and the dynamic pressure depends on mass density of air ρ and mean wind velocity U_∞. The calculation and measurement results are presented in *Fig. 2*. Experimental data is indicated by symbols and the corresponding CFD calculation results by lines. For small wind incident angles (cf. *Fig. 1*) a very good agreement between the data can be observed, for larger angles the drag is slightly overestimated by the calculation. Lift and moment can be very well approximated by linear approximations, the drag is almost constant for small angles.

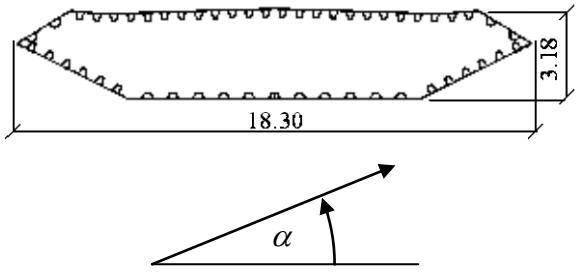

Fig. 1. Deck cross section of Hardanger bridge with definition of wind incident angle

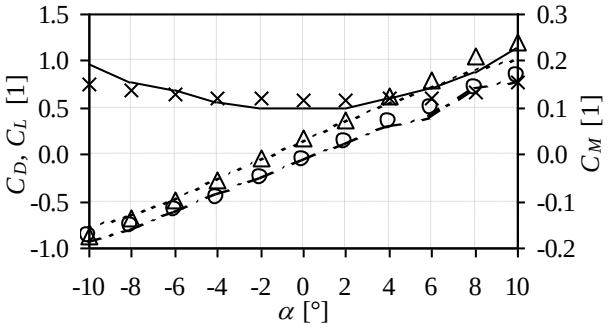

Fig. 2. Steady state coefficients of Hardanger bridge deck: C_D (x), C_L (o) and C_M (Δ)

In the next step, the effects of additional wind guiding vanes and spoilers were investigated. The calculations were performed with a modified cross section layout according to *Fig. 3*. Along the left and right edges additional maintenance rails are installed. Below the deck, there are two wind guiding vanes and one central spoiler to reduce deck vibration due to wind forces. By applying the guiding vanes, two effects could be observed. First a reduction of the lift coefficient of about 30% is detected, cf. *Fig. 4*. Considering the distribution of energy transfer in the frequency domain by inspecting the power spectra of lift force, *Fig. 5*, and overturning moment, *Fig. 6*, it is seen that pronounced peaks are suppressed in the case of wind guiding vanes. This is advantageous both for flutter as well as vortex shedding, because less energy is transferred at certain frequencies. Therefore, the risk and consequences of the lock-in effect can be minimized.

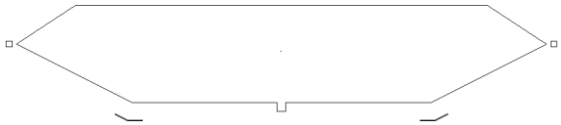

Fig. 3. Cross section with wind guiding vanes and spoiler for Hardanger bridge.

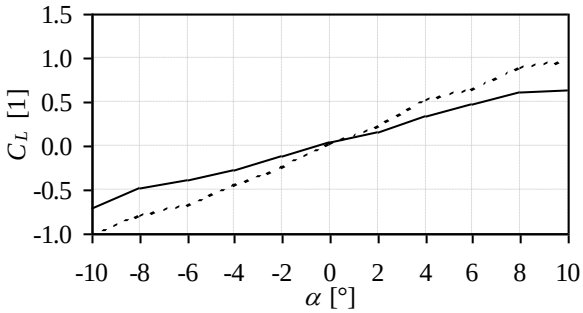

Fig. 4. Lift coefficient for deck with (solid) and without (dashed) wind guiding vanes.

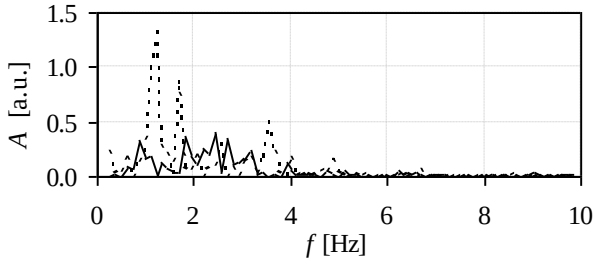

Fig. 5. Lift force power spectrum with (solid) and without (dashed) guiding vanes.

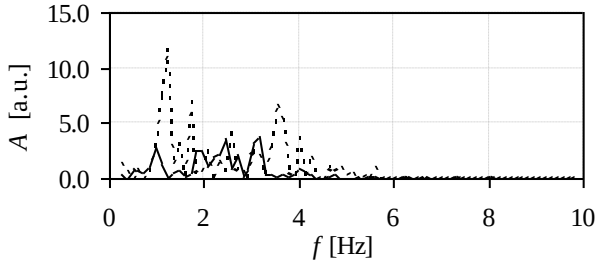

Fig. 6. Moment power spectrum with (solid) and without (dashed) guiding vanes.

Finally the influence of traffic on the aerodynamics of the main girder was investigated. The two driving lanes are loaded with traffic according to the sketch presented in *Fig. 7*. For the CFD calculations three different cases were considered: with both lanes loaded, only with the left lane and only with the right lane. Since the application of traffic causes a symmetry break of the cross section layout, the CFD calculations must be performed for wind coming from the left (-10° to 10°) as well as from the right (170° to 190°). The computed results for the case with both traffic lanes are indicated in *Fig. 8*.

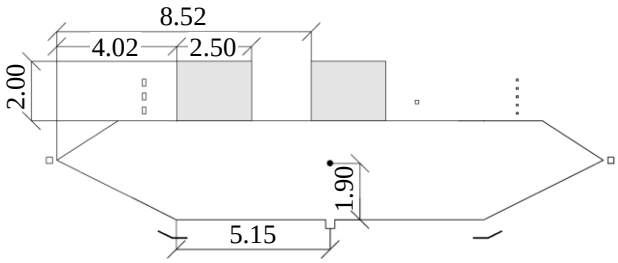

Fig. 7. Cross section for traffic calculation.

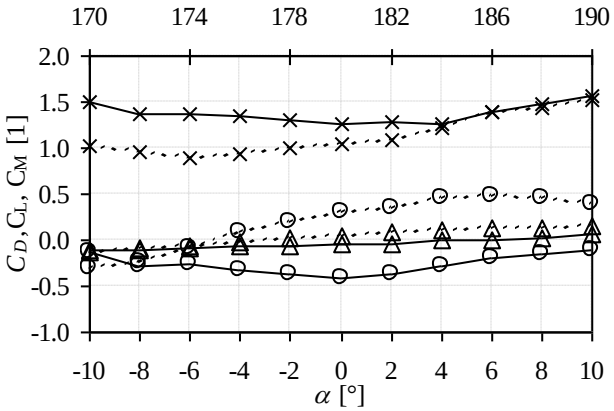

Fig. 8. Steady state coefficients C_D (x), C_L (o) and C_M (Δ) for traffic on both lanes for wind from left (solid) and right (dashed).

Additionally to the investigations for the main deck, wind shadow effect analyses of the used pylon cross sections at different height levels were performed to identify the most critical wind directions.

These investigations were performed with simplified, rectangular shapes of the pylon leg cross sections as indicated in *Fig. 9*. In general, two regimes can be clearly distinguished. One is valid for wind incident angles $\alpha < 50°$. This is the region where pronounced wind shadow effects were calculated. For higher angles, each of the legs can be considered as isolated entity and the resulting coefficients are the same for both legs. In *Fig. 10* this behavior is indicated for the approximate deck position 55 m above ground. At this height the distance D between the pylon legs is approximately 25 m. During the investigation no significant dependence of the wind shadow effect on the leg distance was observed.

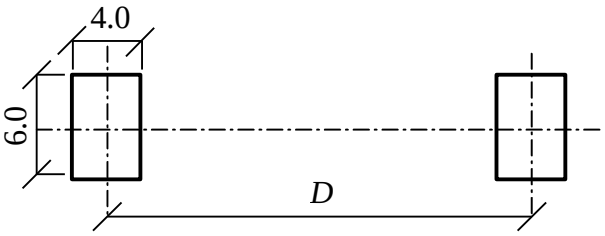

Fig. 9. Cross section model for pylon investigations.

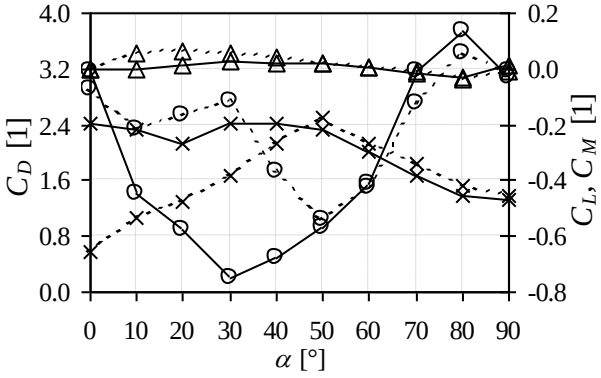

Fig. 10. Steady state coefficients C_D (x), C_L (o) and C_M (Δ) for left (solid) and right (dashed) pylon leg.

3 WIND BUFFETING ANALYSIS

To account for the wind interaction with deck and pylons, the loading was separated into static and dynamic contributions. The static analysis is based on the 10-minute mean wind velocity and the load can be calculated directly from *Eq. (1)* after applying appropriate coordinate transformations between local wind coordinates and bridge coordinates. For the fluctuating wind components the influence can only be estimated by applying statistical methods, because the fluctuations are random themselves. These statistic properties of wind are described by the mean wind velocity, turbulence intensity, power spectral density and wind coherence data. The mean wind and power spectra applied to the Hardanger bridge are indicated in *Fig. 11* and *Fig. 12*, respectively.

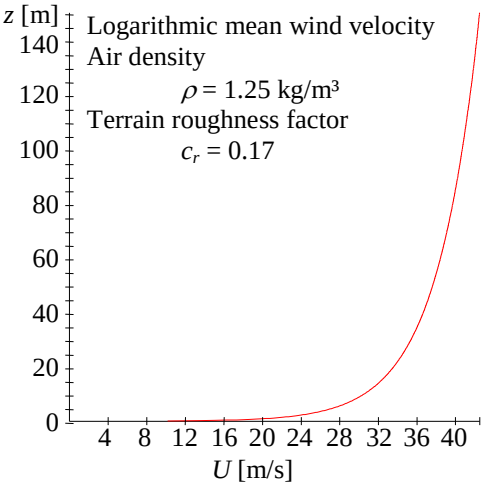

Fig. 11. Mean wind profile.

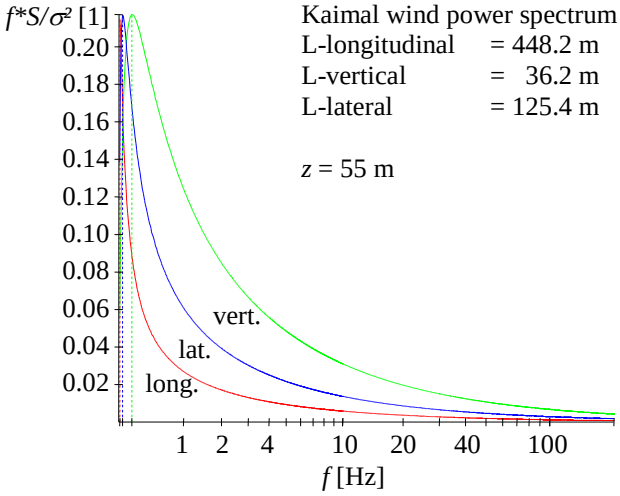

Fig. 12. Power spectra of longitudinal, vertical and lateral fluctuating wind components.

For the further calculation procedure the analysis is performed in modal space and frequency domain. A detailed description about theory of wind buffeting analysis is presented e.g. in [7, 8]. The implementation for the performed analysis is described in [4]. The first step is to split the overall wind force in several contributions according to

$$\begin{pmatrix} D \\ L \\ M \end{pmatrix} = \frac{1}{2}\rho U_\infty^2 \begin{pmatrix} HC_D \\ BC_L \\ B^2 C_M \end{pmatrix}_{\text{st}} + \rho U_\infty \begin{pmatrix} HC_D u + \frac{1}{2}\left(HC'_D - BC_L\right)w \\ BC_L u + \frac{1}{2}\left(BC'_L + HC_D\right)w \\ B^2 C_M u + \frac{1}{2}B^2 C'_M w \end{pmatrix}_{\text{dyn}} - \rho U_\infty \begin{pmatrix} HC_D \dot{r}_z + \frac{1}{2}\left(HC'_D - BC_L\right)\dot{r}_y \\ BC_L \dot{r}_z + \frac{1}{2}\left(BC'_L + HC_D\right)\dot{r}_y \\ B^2 C_M \dot{r}_z + \frac{1}{2}B^2 C'_M \dot{r}_y \end{pmatrix}_{\text{damp}} + \rho U_\infty \begin{pmatrix} \frac{1}{2}HC'_D \vartheta_x \\ \frac{1}{2}BC'_L \vartheta_x \\ \frac{1}{2}B^2 C'_M \vartheta_x \end{pmatrix}_{\text{stiff}} \tag{2}$$

The leading term indicates the static contribution due to mean wind. The second, dynamic term accounts for the forces due to fluctuating wind components *u* (longitudinal) and *w* (transversal). The interaction of the structure and wind is modelled by the so called aerodynamic damping and stiffness which depend on structure displacement, velocity and deflection. These terms can be combined with structural damping and stiffness to yield the system total stiffness and damping. To obtain *Eq. (2)*, it was assumed that the fluctuating components and cross section velocities are small compared to the mean wind velocity, so that all cross-coupling terms of these small contributions can be neglected, cf. also [9].

In the next step, the eigenfrequencies and –modes of the bridge under permanent loading due to self weight and applied static wind load are determined for a modal representation of the dynamic equations. The calculation was performed taking into account non-linear effects by referring to the tangent stiffness in a iterative solution procedure. The undeformed structure and the lowest eigenmodes are presented in *Fig. 13* and *Fig. 14*.

Fig. 13. Structural model of Hardanger bridge.

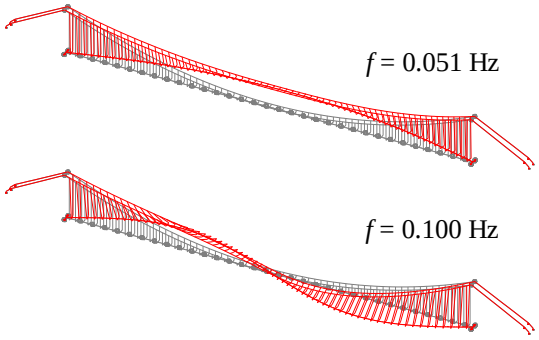

Fig. 14. First two eigenmodes of Hardanger bridge deck.

Finally, a transformation from time domain to frequency domain was performed to solve the equations of motion for each considered eigenmode. By taking into account the wind power spectrum and coherence, a frequency domain representation of the dynamic wind force can be calculated which properly takes into account random wind properties as well as wind cross-section interaction. By combining this excitation spectrum with the mechanical admittance of the structure, which is determined by modal mass, stiffness and damping as well as aerodynamic stiffness and damping, the peak response of each mode can be estimated. The overall response of the structure is obtained by a statistical superposition of all considered eigenmodes.

A comparison of internal forces due to static and dynamic wind contributions is presented in *Fig. 15* and *Fig. 16*. For the present case, the shear forces are of the same magnitude, but the twisting moment is about ten times higher for the fluctuating wind. This difference highlights the importance of such wind investigations.

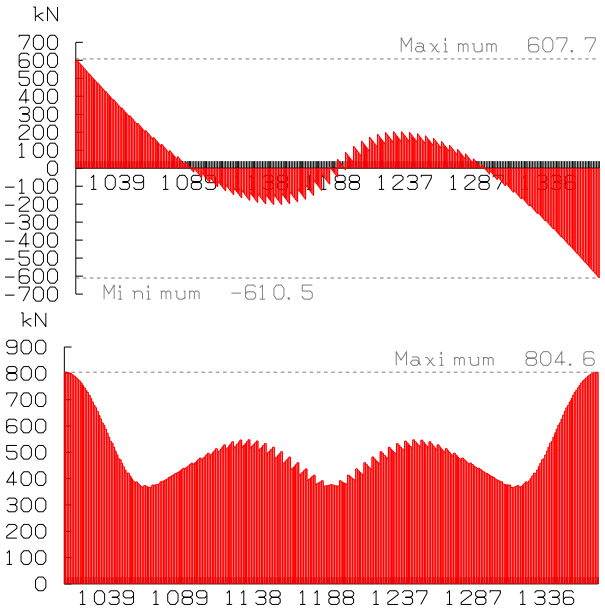

Fig. 15. Comparison of internal shear force due to lateral wind with static (top) and dynamic (bottom) contribution.

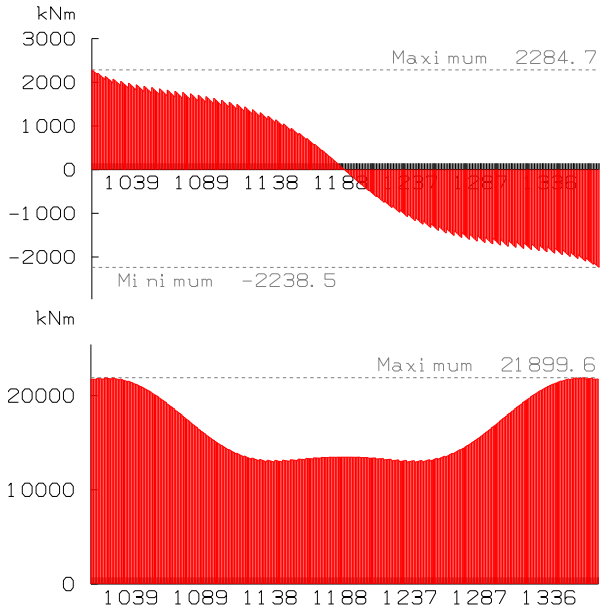

Fig. 16. Comparison of longitudinal twisting moment due to lateral wind with static (top) and dynamic (bottom) contribution.

4 CONCLUSIONS

In this paper the application of comprehensive wind investigation methods to the Hardanger bridge was presented. These methods, which are based on highly sophisticated mathematical models, are becoming more and more a must for the design of long span bridges. This fact was demonstrated by comparing the contributions of static and fluctuating wind forces to the resulting internal forces.

REFERENCES

[1] Morgenthal, G., *Aerodynamic Analysis of Structures Using High-resolution Vortex Particle Methods*, PhD Thesis, University of Cambridge, Cambridge, 2002

[2] Stampler, J., Janjic, D. and Domaingo, A., *Integrated Computer Wind Design for Bridge Engineering*, IABSE Congress, Weimar, 2007.

[3] Beier, M., e.a, *Wind Tunnel Validation of Vortex Method for Aerodynamic Coefficients*, IABSE Congress, Weimar, 2007.

[4] Janjic, D.and Pircher, H., *Consistent Numerical Model for Wind Buffeting Analysis of Long-Span Bridges*, IABSE-Symposium, Shanghai 2004.

[5] Janjic, D., Bokan, H. and Stampler, J., *Computer Aided Design & Erection of Long Suspension Bridges*, IABSE Congress, Weimar, 2007.

[6] B. Lechner, *Aerodynamische Untersuchungen eines Modells der Hardangerbrücke im Windkanal des K+vif mit einer 5-Komponentenwaage*, K+vif, Graz, 2006.

[7] Simiu, E. and Scanlan, R.H., *Wind Effects on Structures: Fundamentals and Application to Design*, New York: John Wiley & Sons, 1996.

[8] Strømmen E.N., *Theory of Bridge Aerodynamics*, Berlin Heidelberg: Springer-Verlag, 2006.

[9] Hjorth-Hansen, E., *Wind Engineering*, lecture notes, University of Trondheim, Norway, 1988.